Supplementary Information

Switchable Ferroelectric Photovoltaic Effects in Epitaxial *h*-$RFeO_3$ Thin Films

Hyeon Han,[a] Donghoon Kim,[a] Sangmin Chae,[b] Jucheol Park,[c] Sang Yeol Nam,[c,d] Mingi Choi,[e] Kijung Yong,[e] Hyo Jung Kim,[b] Junwoo Son,[a] and Hyun Myung Jang*[a]*

[a]Department of Materials Science and Engineering, and Division of Advanced Materials Science, Pohang University of Science and Technology (POSTECH), Pohang 37673, Republic of Korea

[b]Department of Organic Material Science and Engineering, Pusan National University, Busan 46241, Republic of Korea

[c]Gyeongbuk Science & Technology Promotion Center, Gumi Electronics & Information Technology Research Institute, Gumi 39171, Republic of Korea

[d]Department of Materials Science and Engineering, Kumoh National Institute of Technology, Gumi 39177, Republic of Korea

[e]Department of Chemical Engineering, Pohang University of Science and Technology (POSTECH), Pohang 37673, Republic of Korea

*** Corresponding Author**

E-mail: jwson@postech.ac.kr (J. Son) or hmjang@postech.ac.kr (H. M. Jang)

Section 1. Supplementary Figures & Tables

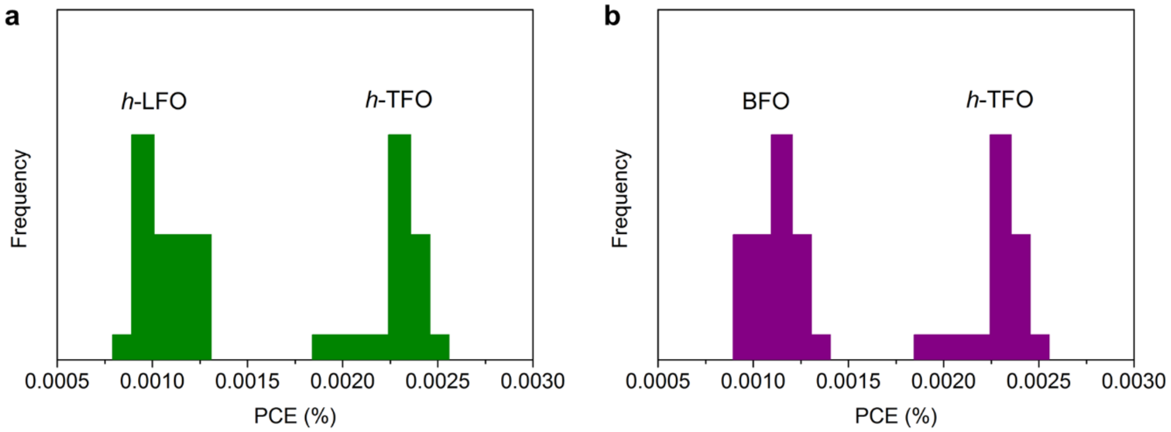

Figure S1. Distribution of power conversion efficiency (PCE) for (a) *h*-TFO and *h*-LFO devices, and (b) *h*-TFO and BFO devices. N = 10 samples are measured for each devices.

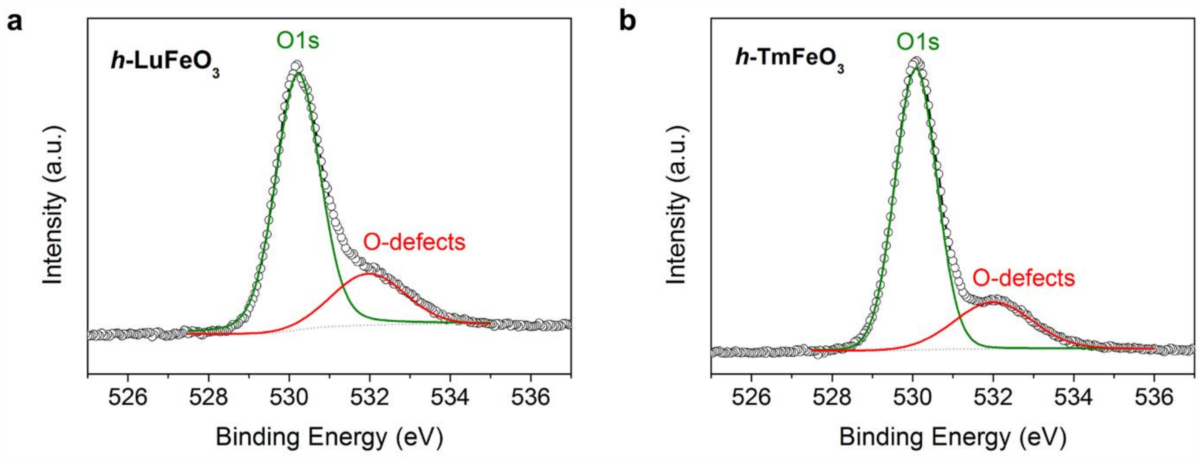

Figure S2. X-ray photoelectron spectra (XPS) of the (a) *h*-LFO and (b) *h*-TFO thin films. The deconvolution of the O1s line results in two peaks of the oxygen (green line) in the *h*-RFO lattice and the oxygen defects (red line).

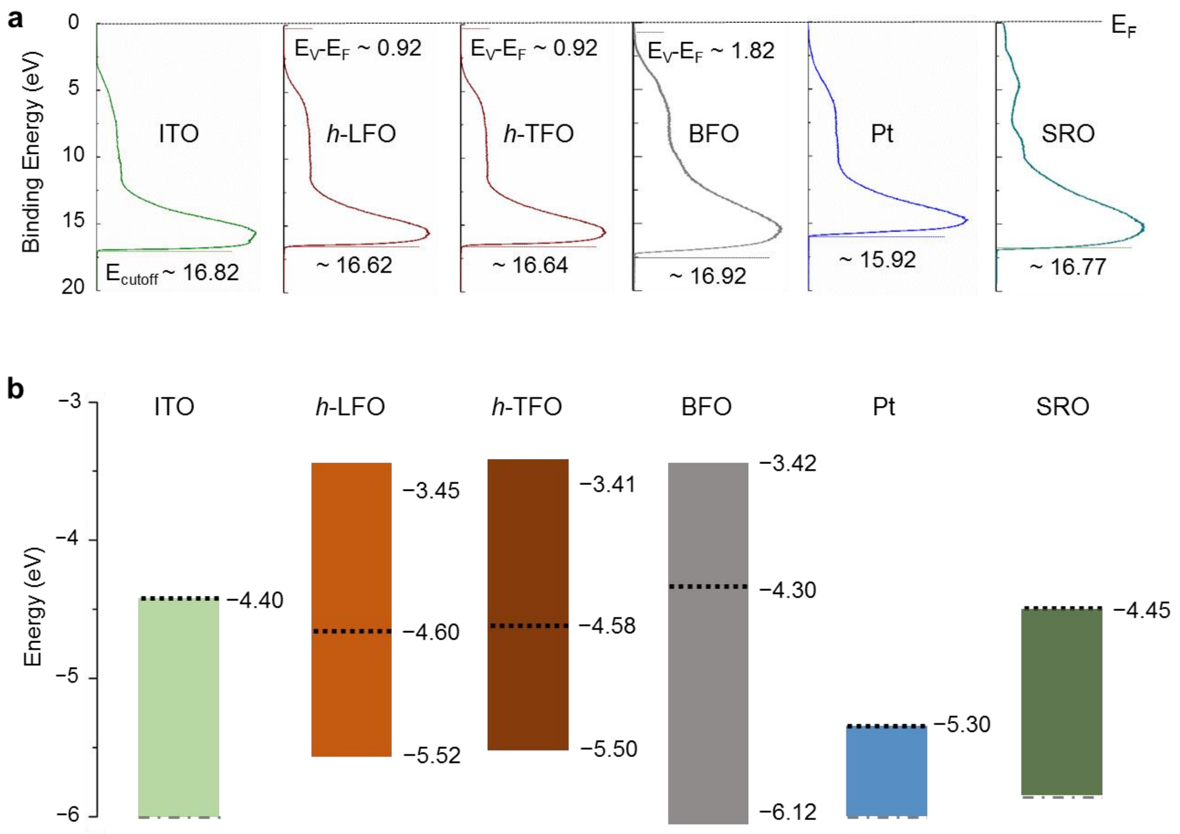

Figure S3. (a) UPS spectra of ITO, *h*-LFO, *h*-TFO, BFO, Pt, and SRO (from the left to the right-hand-side). A low binding-energy region is for the valance-band determination and a high binding-energy region for the work-function determination. (b) An energy level diagram showing the conduction-band minimum, valence-band maximum, and the Fermi level (a dashed line) of each constituting materials.

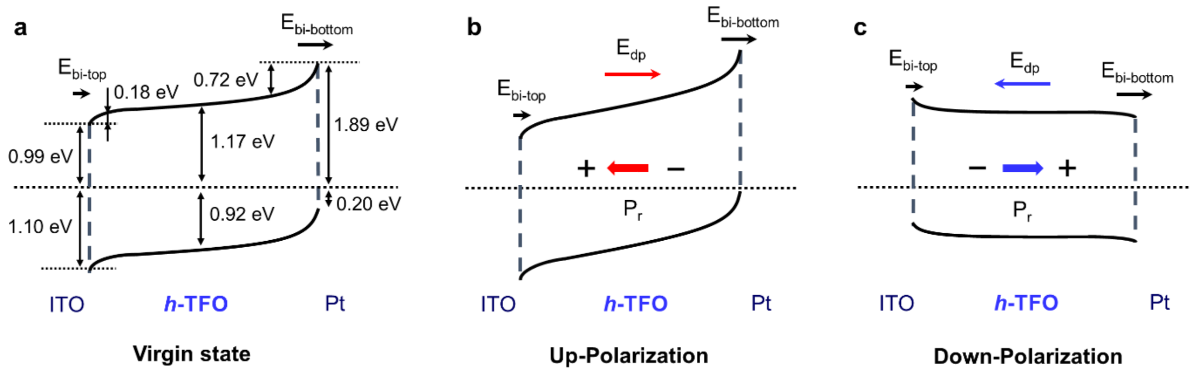

Figure S4. Modulated energy band diagrams of the ITO/*h*-TFO/Pt device. From the left, the virgin state (without poling), the up-polarization state (under upward poling), and the down-polarization state (under downward poling) are shown.

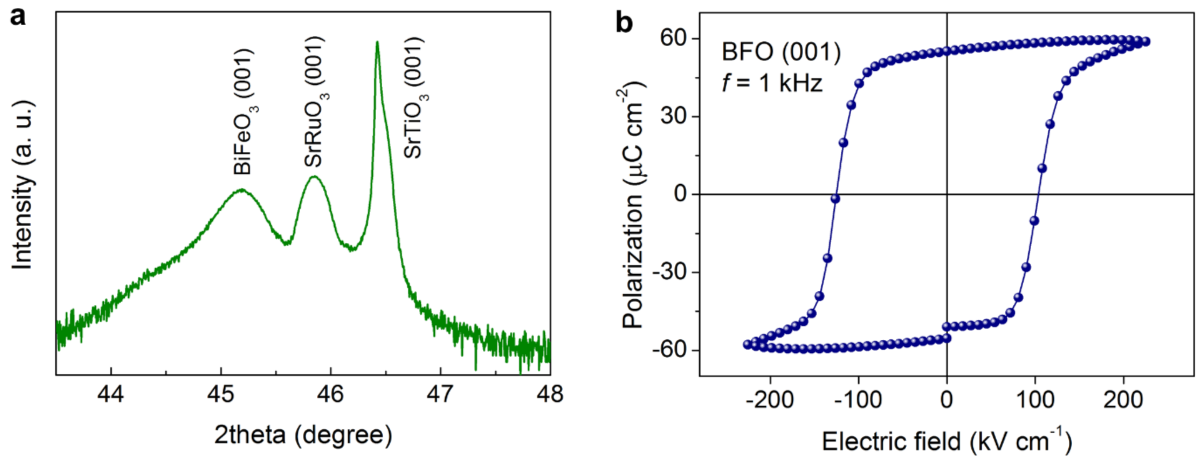

Figure S5. (a) Theta−2theta (*θ−2θ*) X-ray diffraction (XRD) pattern of the preferential [001]-oriented $BiFeO_3$ thin film grown on $SrRuO_3$ (001)/$SrTiO_3$ (001) substrate. (b) A polarization-electric field (*P*-*E*) hysteresis loop of the 250-nm-thick (001)-oriented $BiFeO_3$ (BFO) layer obtained at 300 K, 1 kHz.

Section 2. Interpretation of the thickness-dependent V_{oc}

As shown in Fig. 4a and 4b, the photocurrent tends to increase with decreasing film thickness. This is because both the depolarization field effect and the Schottky-junction barrier effect increase with decreasing film thickness. However, similar to the previously reported paper (*Chem. Mater.* 2015, **27**, 7425), V_{oc} does not change significantly for the film thickness above ~150 nm. In other words, the depolarization field weakens with increasing film thickness. According to the **bulk** photovoltaic (BPV) effect, on the contrary, V_{oc} increases with the film thickness (or with the electrode distance), according to the following simple equation (*Nat. Nanotech.* 2010, **5**, 143–147; *J. Mater. Chem. A* 2014, **2**, 6027)**:** $V_{OC} = Ed$. Therefore, it is considered that the thickness dependent V_{oc} **is a consequence of the trade-off** between the depolarization field effect and the BPV effect.

Furthermore, *S. Y. Yang et al.* described that V_{oc} essentially remains constant even if the film thickness increases further because the photovoltaic response primarily occurs within a depletion layer having the thickness of several hundred nano-meters (*Appl. Phys. Lett.* 2009, **95**, 062909).